J|A|C|S ARTICLES

Published on Web 03/16/2009

Hydrogen- and Oxygen-Driven Interconversion between Imido-Bridged Dirhodium(III) and Amido-Bridged Dirhodium(II) Complexes

Koji Ishiwata, Shigeki Kuwata,* and Takao Ikariya*

Department of Applied Chemistry, Graduate School of Science and Engineering, Tokyo Institute of Technology, O-okayama, Meguro-ku, Tokyo 152-8552, Japan

Received January 27, 2009; E-mail: skuwata@apc.titech.ac.jp; tikariya@apc.titech.ac.jp

Abstract: The reaction of $[Cp^*RhCl_2]_2$ ($Cp^* = \eta^5$-$C_5(CH_3)_5$) with 2 equiv of *p*-toluenesulfonamide in the presence of KOH resulted in the formation of the sulfonylimido-bridged dirhodium(III) complex $[(Cp^*Rh)_2(\mu\text{-}NTs)_2]$ (**1a**; Ts = $SO_2C_6H_4CH_3$-*p*). The imido complex **1a** reacted with hydrogen donors such as H_2 and 2-propanol to give the sulfonylamido-bridged dirhodium(II) complex $[(Cp^*Rh)_2(\mu\text{-}NHTs)_2]$ (**2**). Treatment of the (amido)rhodium(II) complex **2** with O_2 regenerated the (imido)rhodium(III) complex **1a**. Complex **1a** also underwent reversible protonation to afford the cationic amido- and imido-bridged dirhodium(III) complex $[(Cp^*Rh)_2(\mu\text{-}NHTs)(\mu\text{-}NTs)]^+$ (**4**), which further reacted with H_2 or 2-propanol to give the (hydrido)bis(amido)dirhodium(III) complex $[(Cp^*Rh)_2(\mu\text{-}H)(\mu\text{-}NHTs)_2]^+$ (**5**). On the basis of DFT calculations and experimental results using **4** and **5**, the reaction of **1a** with H_2 proved to proceed via heterolytic cleavage of H_2 assisted by the sulfonyl oxygen atom followed by proton migration from the metal center. Furthermore, the redox interconversion between **1a** and **2** was applied to catalytic aerobic oxidation of H_2 and an alcohol by using **1a** as a well-defined dinuclear catalyst. The iridium complex $[(Cp^*Ir)_2(\mu\text{-}NTs)_2]$ (**1b**) as well as a rhodium complex $[Cp^*RhCl_2]_2$ without bridging imido ligands did not catalyze these aerobic oxidation reactions.

Introduction

Metal-mediated interconversion of H_2 into two protons and two electrons has been studied extensively in relation to the hydrogen metabolism, electrocatalysts for fuel cells, and photocatalyic water splitting.[1] Hydrogenase enzymes are known to catalyze this interconversion with quite high efficiency.[2] Currently accepted mechanisms of the biological H_2 oxidation involve ligand-assisted heterolysis of H_2 into a proton and metal hydride, followed by two-electron oxidation of the hydride to produce the second proton. In this connection, numerous examples of the heterolytic cleavage of H_2 by metal−ligand (Scheme 1, a) or metal-external base (b) cooperation[1,3−7] have been accumulated. They are, however, rarely linked with the subsequent proton liberation from the resultant metal hydride, which completes the H_2 oxidation.[5−7]

We have investigated the bifunctional catalysis of chelate amido complexes featuring the amido−amine interconversion as exemplified in eq 1.[3,8,9] In the catalysis, dihydrogen as well as other hydrogen donors reacts with the coordinatively unsaturated amido complex to afford the saturated hydrido−amine complex thanks to the cooperation of the Lewis acidic metal center and Brønsted basic NH group; the hydrido−amine complex transfers a proton and hydride to unsaturated substrates such as ketones, regenerating the amido complex. We reasoned that both the heterolysis of H_2 and oxidation of the hydride shown in Scheme 1a would be promoted by sulfonylimido-bridged dinuclear complexes bearing a multimetallic structure

Scheme 1

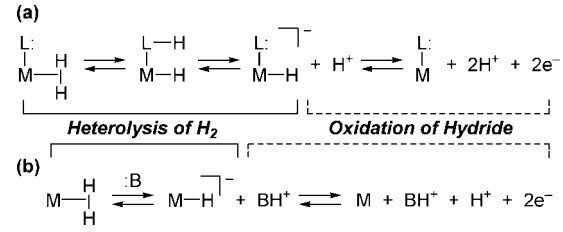

(1) (a) Kubas, G. J. *Chem. Rev.* **2007**, *107*, 4152. (b) Tye, J. W.; Darensbourg, M. Y.; Hall, M. B. In *Activation of Small Molecules*; Tolman, W. B., Ed.; Wiley-VCH: Weinheim, Germany, 2006; pp 121−158. (c) Morris, R. H. In *Concepts and Models in Bioinorganic Chemistry*; Kraatz, H.-B., Metzler-Nolte, N., Eds.; Wiley-VCH; Weinheim, Germany, 2006; pp 331−362.

(2) (a) Fontecilla-Camps, J. C.; Volbeda, A.; Cavazza, C.; Nicolet, Y. *Chem. Rev.* **2007**, *107*, 4273. (b) De Lacey, A. L.; Fernández, V. M.; Rousset, M.; Cammack, R. *Chem. Rev.* **2007**, *107*, 4304. (c) Lubitz, W.; Reijerse, E.; van Gastel, M. *Chem. Rev.* **2007**, *107*, 4331.

(3) Ito, M.; Ikariya, T. *Chem. Commun.* **2007**, 5134.

(4) (a) Brown, S. D.; Mehn, M. P.; Peters, J. C. *J. Am. Chem. Soc.* **2005**, *127*, 13146. (b) Matsumoto, T.; Nakaya, Y.; Tatsumi, K. *Angew. Chem., Int. Ed.* **2008**, *47*, 1913. (c) Ohki, Y.; Sakamoto, M.; Tatsumi, K. *J. Am. Chem. Soc.* **2008**, *130*, 11610.

(5) (a) Hembre, R. T.; McQueen, J. S.; Day, V. W. *J. Am. Chem. Soc.* **1996**, *118*, 798. (b) Curtis, C. J.; Miedaner, A.; Ciancanelli, R.; Ellis, W. W.; Noll, B. C.; Rakowski DuBois, M.; DuBois, D. L. *Inorg. Chem.* **2003**, *42*, 216. (c) Wilson, A. D.; Shoemaker, R. K.; Miedaner, A.; Muckerman, J. T.; DuBois, D. L.; Rakowski DuBois, M. *Proc. Natl. Acad. Sci. U.S.A.* **2007**, *104*, 6951. (d) Rakowski DuBois, M.; DuBois, D. L. *C. R. Chimie* **2008**, *11*, 805. (e) Ringenberg, M. R.; Kokatam, S. L.; Heiden, Z. M.; Rauchfuss, T. B. *J. Am. Chem. Soc.* **2008**, *130*, 788. (f) Matsumoto, T.; Nakaya, Y.; Itakura, N.; Tatsumi, K. *J. Am. Chem. Soc.* **2008**, *130*, 2458. (g) Rakowski DuBois, M.; DuBois, D. L. *Chem. Soc. Rev.* **2009**, *38*, 62.

(6) Laurie, J. C. V.; Duncan, L.; Haltiwanger, R. C.; Weberg, R. T.; Rakowski DuBois, M. *J. Am. Chem. Soc.* **1986**, *108*, 6234.

(7) Matsumoto, T.; Kure, B.; Ogo, S. *Chem. Lett.* **2008**, *37*, 970.

suitable for the electron reservoir in addition to unsaturated and bifunctional metal−nitrogen moieties.[10,11] We report here the reactions of the sulfonylimido-bridged dirhodium(III) complex [(Cp*Rh)$_2$(μ-NTs)$_2$] (**1a**; Cp* = η^5-C$_5$(CH$_3$)$_5$, Ts = SO$_2$C$_6$H$_4$CH$_3$-*p*) with H$_2$ and 2-propanol as a hydrogen donor, leading to two-electron reduction of the dirhodium core and formation of two Brønsted acidic amido ligands. The resulting sulfonylamido-bridged dirhodium(II) complex [(Cp*Rh)$_2$(μ-NHTs)$_2$] (**2**) readily reacted with O$_2$ to regenerate **1a**. The catalytic application to aerobic oxidation of H$_2$ and alcohols is also described.

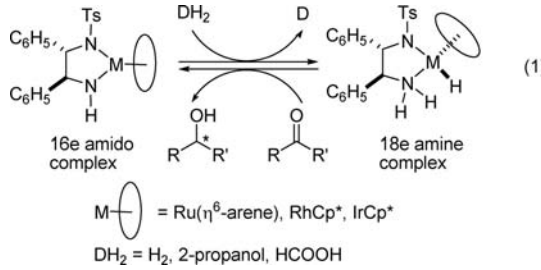

Results and Discussion

Synthesis of Imido-Bridged Dirhodium(III) Complex 1a and Its Reaction with H$_2$. The bis(imido)-bridged dirhodium(III) complex **1a** was obtained by using the synthetic protocol for the iridium analogue [(Cp*Ir)$_2$(μ-NTs)$_2$] (**1b**).[10] Thus, the reaction of [Cp*RhCl$_2$]$_2$ with 2 equiv of TsNH$_2$ in the presence of KOH smoothly took place to afford **1a** in excellent yield (eq 2). The coordinatively unsaturated, yet air- and moisture-stable complex **1a** has been characterized by ^{1}H NMR spectroscopy and elemental analysis as well as X-ray crystallography.[12]

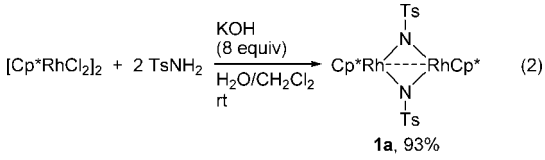

The bis(imido)-bridged dirhodium(III) complex **1a** reacted with H$_2$ (1 atm) in dichloromethane for 24 h at room temperature to afford the bis(amido)-bridged dirhodium(II) complex **2** in 82% yield as shown in Scheme 2. The NH signals at δ 5.46 and 2.53 in the ^{1}H NMR spectrum of **2** were identified by their exchange with added D$_2$O. An X-ray diffraction analysis of **2**·TsNH$_2$, which has been obtained by recrystallization of **2** in the presence of TsNH$_2$, revealed that the presence of intra- and intermolecular hydrogen bonds between the amido protons and the sulfonyl O atoms (Figure 1). The Rh$_2$N$_2$ ring is puckered with the dihedral angle around the Rh−Rh vector of 106.3(4)°.

Scheme 2

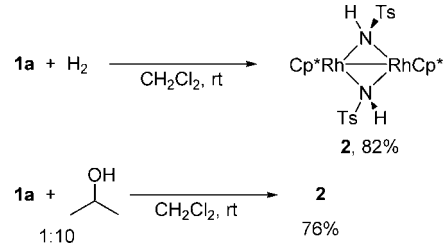

The mutually *anti*-orientation of the NH group with respect to the Rh$_2$N$_2$ face contrasts with the *syn*-orientation in the recently reported phenylamido analogue [(Cp*Rh)$_2$(μ-NHC$_6$H$_5$)$_2$] (**3**).[13] The Rh−Rh distance in **2** is much shorter than that in **1a** (2.6004(12) vs 2.7992(4)[12b] Å) and comparable to that in **3** (2.6097(9) Å)[13] in agreement with the presence of a Rh(II)−Rh(II) single bond. The tetrahedral configuration of the bridging nitrogen atoms is evidenced by the sum of the Rh−N−Rh and two Rh−N−S angles (327.6°, mean).

In this reaction, H$_2$ is formally converted into two amido protons and two electrons for the reduction of the dirhodium(III) core in **1a**. Such H$_2$ oxidation on dinuclear platforms remains quite rare.[1,6,7,14] Rakowski DuBois and co-workers reported that the reaction of a dimolybdenum(IV) complex [(Cp′Mo)$_2$(μ-S$_2$CH$_2$)(μ-S)(μ-SCH$_3$)]$^+$ (Cp′ = η^5-C$_5$H$_4$CH$_3$) with H$_2$ in the presence of pyridine results in two-electron reduction of the dimolybdenum core and formation of pyridinium and hydrosulfido protons.[6] They also revealed that hydrogenation of the related dimolybdenum(IV) complex [(Cp′Mo)$_2$(μ-S)$_2$(μ-η^2:η^2-S$_2$)] leads to protonation and reduction of the disulfido ligand to afford the bis(hydrosulfido)-bridged dimolybdenum(IV) complex [(Cp′Mo)$_2$(μ-S)$_2$(μ-SH)$_2$]; these complexes serve as hydrogenation catalysts for imines and azobenzene.[15] It is noteworthy that different reactivities are observed for some dinuclear complexes that are formally isoelectronic with **1a**: the sulfido-bridged dirhodium(III) complex [{(triphos)Rh}$_2$(μ-S)$_2$]$^{2+}$ (triphos = {(C$_6$H$_5$)$_2$PCH$_2$}$_3$CCH$_3$) undergoes reversible, double heterolysis of H$_2$ to give the (hydrido)(hydrosulfido)dirhodium(III) complex [{(triphos)RhH}$_2$(μ-SH)$_2$]$^{2+}$,[16] whereas the phenylimido-bridged diiridium(III) complex [(Cp*Ir)$_2$(μ-NC$_6$H$_5$)$_2$] reacts with H$_2$ under more forcing conditions to liberate aniline.[17]

The amido complex **2** was also obtained upon treatment of **1a** with an excess of 2-propanol (Scheme 2). The generation of

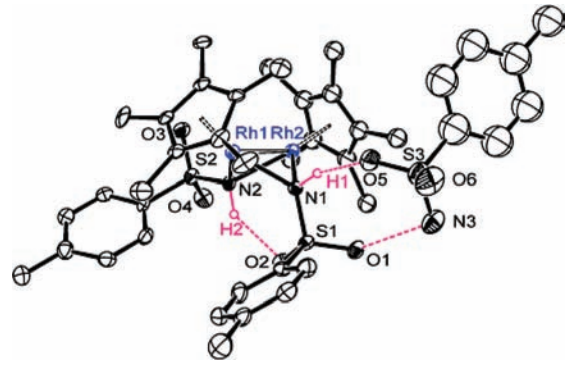

Figure 1. Structure of **2**·TsNH$_2$ with thermal ellipsoids at the 30% probability level. Hydrogen atoms except for the μ-NHTs protons are omitted for clarity. Selected interatomic distances (Å): Rh1−Rh2, 2.6004(12); Rh1−N1, 2.109(8); Rh1−N2, 2.110(7); Rh2−N1, 2.137(8); Rh2−N2, 2.121(9); N1−S1, 1.619(8); N2−S2, 1.628(8); O1−N3, 2.951(13); O5−H1, 2.203; O2−H2, 2.056.

(8) Ikariya, T.; Blacker, A. J. *Acc. Chem. Res.* **2007**, *40*, 1300.
(9) (a) Hasegawa, Y.; Watanabe, M.; Gridnev, I. D.; Ikariya, T. *J. Am. Chem. Soc.* **2008**, *130*, 2158. (b) Ito, M.; Osaku, A.; Kobayashi, C.; Shiibashi, A.; Ikariya, T. *Organometallics* **2009**, *28*, 390. (c) Shirai, S.; Nara, H.; Kayaki, Y.; Ikariya, T. *Organometallics* **2009**, *28*, 802. (d) Ito, M.; Koo, L.-W.; Himizu, A.; Kobayashi, C.; Sakaguchi, A.; Ikariya, T. *Angew. Chem., Int. Ed.* **2009**, *48*, 1324.
(10) (a) Ishiwata, K.; Kuwata, S.; Ikariya, T. *Organometallics* **2006**, *25*, 5847. (b) Ishiwata, K.; Kuwata, S.; Ikariya, T. *Dalton Trans.* **2007**, 3606.
(11) Arita, H.; Ishiwata, K.; Kuwata, S.; Ikariya, T. *Organometallics* **2008**, *27*, 493.
(12) (a) Just around the same time of the submission, Tejel and co-workers[12b] independently reported an alternative access to **1a** along with its crystal structure. We thus omitted the X-ray structure of **1a**. (b) Tejel, C.; Ciriano, M. A.; Jiménez, S.; Passarelli, V.; López, J. A. *Inorg. Chem.* **2008**, *47*, 10220.

Scheme 3

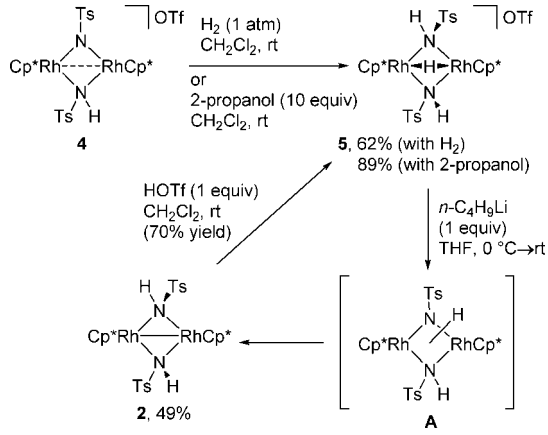

two NH protons associated with two-electron reduction of the metal center strongly contrasts with the conventional dehydrogenation of primary and secondary alcohols by unsaturated mononuclear amido complexes,[8] which leads to the formation of hydrido−amine complexes without formal reduction of the metal. Notably, the corresponding iridium complex **1b**[10] was inert to both H_2 and 2-propanol even under more forcing conditions.

Protonation, Hydrogenation, and Deprotonation Network of Amido- and Imido-Bridged Complexes. As in the case of the iridium congener **1b**,[10a] the rhodium complex **1a** underwent *N*-protonation with an equimolar amount of triflic acid to give the cationic amido- and imido-bridged dirhodium complex **4** despite the presence of the electron-withdrawing sulfonyl group on the imido nitrogen (eq 3). The ^{1}H NMR spectrum of **4** exhibits an NH signal at δ 8.46, while the IR spectrum shows an NH band at 3160 cm^{-1}. The Brønsted acidity of the NH proton in **4** was evidenced by facile deprotonation with KOH to regenerate the parent bis(imido)-bridged complex **1a** in good yield.

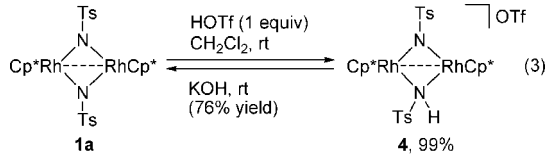

(3)

In contrast to the reaction of **1a** with H_2, simple heterolysis of H_2 took place when the cationic (amido)(imido)dirhodium(III) complex **4** was treated with H_2, giving the (hydrido)bis(amido)dirhodium(III) complex **5** (Scheme 3). 2-Propanol also worked as a hydrogen donor to provide **5**. The ^{1}H NMR spectrum of **5** exhibits a triplet ascribed to the bridging hydrido

Scheme 4

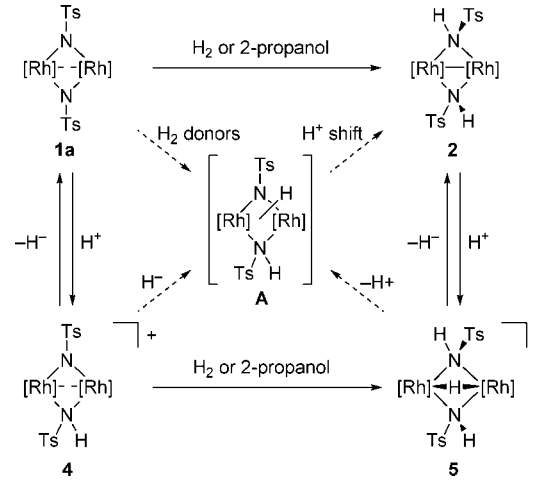

ligand at δ −9.20 ($^1J_{RhH}$ = 23.3 Hz) as well as two NH singlets at δ 6.54 and 5.58, which indicate the *anti* orientation of the two bridging amido ligands in **5**. As expected, reversible protonation of the bis(amido)dirhodium(II) complex **2** provided an alternative route to **5**. Since only the amido protons in **5** undergo H−D exchange upon treatment with D_2O, deprotonation of **5** to **2** would take place by the initial loss of the NH proton to give the hydrido−amido−imido complex **A** as a possible intermediate. A subsequent proton shift from the metal center to the Brønsted basic imido nitrogen would afford **2** with formal reduction of $Rh(III)_2$ to $Rh(II)_2$. The spontaneous proton migration suggests that the relative order of the Brønsted basicity of the metal center and imido nitrogen could be affected by slight structural changes such as the net charge of the complex. We have recently observed a similar proton migration in the mono(sulfonylimido)-bridged diiridium complex [Cp*IrCl(μ-H)(μ-NMs)IrCp*] (Ms = SO_2CH_3), which is triggered by the coordination of carbon monoxide.[11] In line with the facile proton shift, hydride addition to **4** with an equimolar amount of $LiBH(C_2H_5)_3$ also gave the bis(amido) complex **2** immediately. These observations, summarized in Scheme 4, imply that the intermediate **A** may also be generated by the heterolysis of H_2, as well as dehydrogenation of 2-propanol, on **1a**.

DFT Calculations on Reaction of Bis(imido)-Bridged Complex with H_2. To gain more insight into the reaction mechanism of **1a** with H_2, we investigated the reaction pathway of the mesylimido analogue of **1a** [(Cp*Rh)$_2$(μ-NMs)$_2$] (**1a′**) and H_2 by using DFT calculations. We considered the following four possible routes: heterolysis of H_2 at the Rh−N bond followed by proton migration from the Rh atom to the imido nitrogen (Path 1), heterolysis of H_2 assisted by the sulfonyl oxygen followed by proton migration from the Rh atom to the imido nitrogen (Path 2), direct addition of H_2 to the two imido nitrogens without H_2-coordination to the metal (Path 3),[18] and, finally, oxidative addition of H_2 to the Rh atom(s) followed by double proton migration from the rhodium to the imido nitrogens (Path 4). Paths 1 and 2 involve the heterolysis of H_2 to give the hydrido−amido−imido intermediate **A**, while Paths 3 and 4 do not. The calculated energies of the transition states and intermediates in these reaction pathways are summarized in Table 1 and Figure 2.

(13) Takemoto, S.; Otsuki, S.; Hashimoto, Y.; Kamikawa, K.; Matsuzaka, H. *J. Am. Chem. Soc.* **2008**, *130*, 8904.
(14) (a) Oro, L. A.; Sola, E. In *Recent Advances in Hydride Chemistry*; Peruzzini, M., Poli, R., Eds.; Elsevier: Amsterdam, The Netherlands, 2001; pp 299−327. (b) Linck, R. C.; Pafford, R. J.; Rauchfuss, T. B. *J. Am. Chem. Soc.* **2001**, *123*, 8856.
(15) (a) Rakowski DuBois, M. In *Catalysis by Di- and Polynuclear Metal Cluster Complexes*; Adams, R. D., Cotton, F. A., Eds.; Wiley-VCH: New York, 1998; pp 127−143. (b) Rakowski DuBois, M. *Chem. Rev.* **1989**, *89*, 1.
(16) (a) Bianchini, C.; Mealli, C.; Meli, A.; Sabat, M. *Inorg. Chem.* **1986**, *25*, 4617. (b) Ienco, A.; Calhorda, M. J.; Reinhold, J.; Reineri, F.; Bianchini, C.; Peruzzini, M.; Vizza, F.; Mealli, C. *J. Am. Chem. Soc.* **2004**, *126*, 11954.
(17) Dobbs, D. A.; Bergman, R. G. *Organometallics* **1994**, *13*, 4594.
(18) (a) Collman, J. P.; Slaughter, L. M.; Eberspacher, T. A.; Strassner, T.; Brauman, J. I. *Inorg. Chem.* **2001**, *40*, 6272. (b) Dehestani, A.; Lam, W. H.; Hrovat, D. A.; Davidson, E. R.; Borden, W. T.; Mayer, J. M. *J. Am. Chem. Soc.* **2005**, *127*, 3423.

Table 1. Calculated Relative Zero-Point Energies (ΔE_0), Enthalpies (ΔH), and Free Energies (ΔG) in the Reaction Pathways of **1a′** with H_2

Path 1		**GS+H_2**	**GS1-1**	**TS1-1**	**GS2-1**	**TS2-1**	**GS3-1**	**TS3-1**	**GS4-1**	**GS4**
	ΔE_0	0.00	0.41	20.50	20.89	26.01	–1.38	4.78	–28.96	–34.70
	ΔH	0.00	0.21	19.52	19.89	24.35	–2.84	3.09	–30.38	–35.98
	ΔG	0.00	5.46	27.22	26.51	31.99	4.90	11.51	–22.54	–29.26
Path 2		**GS+H_2**	**GS1-2**	**TS1-2**	**GS2-2**	**TS2-2**	**GS3-2**	**TS3-2**		**GS4**
	ΔE_0	0.00	8.21	21.59	20.02	20.97	–7.34	6.64		–34.70
	ΔH	0.00	8.58	20.68	18.83	19.35	–8.83	5.36		–35.98
	ΔG	0.00	10.40	26.33	25.68	27.14	–1.40	12.11		–29.26
Path 3		**GS+H_2**	**GS1-1**			**TS-NN**			**GS4-1**	**GS4**
	ΔE_0	0.00	0.41			33.25			–28.96	–34.70
	ΔH	0.00	0.21			31.63			–30.38	–35.98
	ΔG	0.00	5.46			39.85			–22.54	–29.26

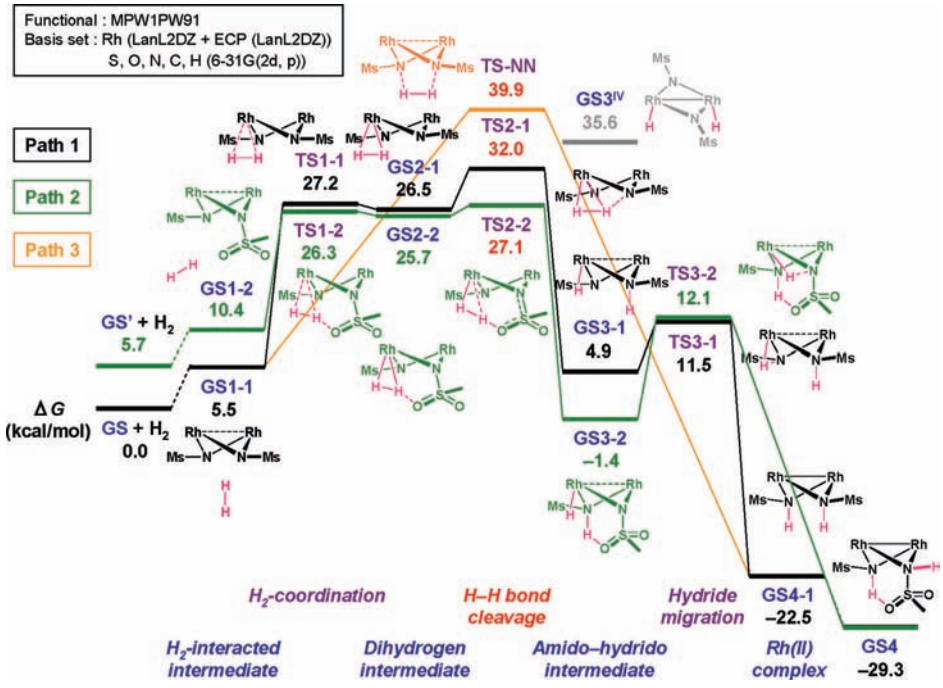

Figure 2. Energy diagrams for the reaction pathways of **1a′** with H_2.

Path 1 starts with the coordination of H_2 to one of the two Rh atoms (**TS1-1**). The η^2-H_2 intermediate **GS2-1** undergoes a proton shift from the dihydrogen ligand to the imido nitrogen (**TS2-1**) to give the hydrido−amido intermediate **GS3-1**. Subsequent proton migration from the Rh atom to the other imido nitrogen (**TS3-1**) leads to the formation of *syn*-bis(amido) intermediate **GS4-1**, which would isomerize to the *anti*-bis(amido) structure **GS4** corresponding to **2a**, being more stable by 6.72 kcal/mol than **GS4-1**.

In Path 2, the reaction is triggered by coordination of H_2 (**TS1-2**) to a less stable *anti*-bis(imido) conformer of **1a′** (**GS′**) obtained by rotation of one of the N−S bonds linked with the inversion of the imido nitrogen. The η^2-H_2 intermediate **GS2-2** undergoes a proton shift from the dihydrogen ligand to the sulfonyl oxygen (**TS2-2**), followed by a proton relay from the sulfonyl oxygen to the opposite side of the imido nitrogen. The latter process proceeds via (i) elongation of the S−O bond and shortening of the H−O distance (**UG1**; Figure 3), (ii) rotation of the N−S bond (**UG2**), and (iii) folding of the Rh_2N_2 ring to transfer the OH proton to the imido nitrogen (**UG3**); these are neither stable intermediates nor transition states. The resultant hydrido−amido intermediate **GS3-2** undergoes proton migration from the Rh atom to the imido nitrogen (**TS3-2**) to afford the *anti*-bis(amido) structure **GS4** corresponding to **2a**. The activation energy for the heterolysis assisted by the sulfonyl O atom through a six-membered transition state **TS2-2** (Chart 1a) proved to be smaller by 4.85 kcal/mol than that for the direct proton shift from the η^2-H_2 ligand to the bridging imido nitrogen (**TS2-1**, Chart 1b).

Path 3 involves concerted [3 + 2] scission of H_2[18] at the imido ligands, which directly gives the *syn*-bis(amido) intermediate **GS4-1** common to Path 1. The activation energy for this process,

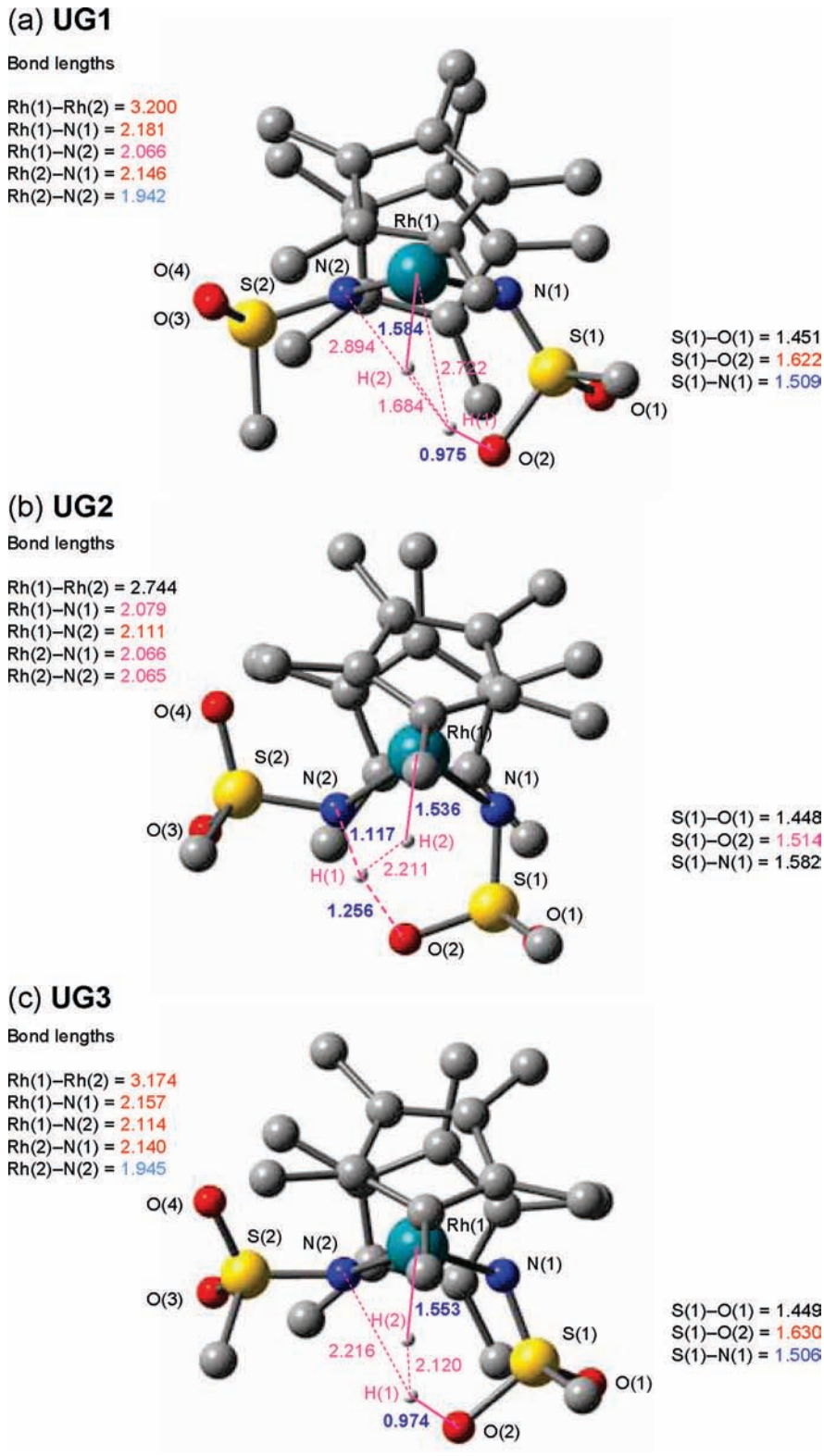

Figure 3. Geometries involved in the proton relay from the sulfonyl oxygen atom (**TS2-2**) to the bridging nitrogen atom (**GS3-2**) in Path 2 (Figure 2). Methyl hydrogens are omitted for clarity. Interatomic distances are in Å.

via a transition state **TS-NN**, was estimated to be as large as 39.85 kcal/mol.

For Path 4, oxidative addition of H_2 to a single metal center and that to the dinuclear core should be considered. Dinuclear oxidative addition of H_2 would afford the $Rh(IV)_2$ dihydrido complex $[(Cp^*RhH)_2(\mu\text{-}NMs)_2]$ (**GS3^{IV}**) as a primary product. The calculated energy of this dihydride intermediate, however, proved to be very high (35.56 kcal/mol). On the other hand, structural optimization of the Rh(III)/Rh(V) dihydride complex $[Cp^*RhH_2(\mu\text{-}NMs)_2RhCp^*]$, which would be generated by oxidative addition to one of the two Rh atom, resulted in the convergence to the η^2-H_2 intermediate **GS2-1**.

Chart 1

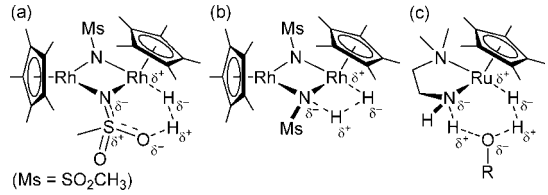

Scheme 5

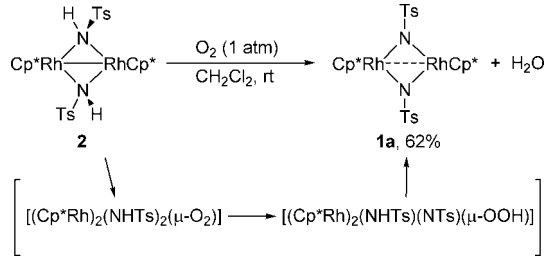

We thus concluded that heterolytic cleavage of H_2 assisted by the sulfonyl O atom (Path 2) is the most energetically favorable pathway among the four possible routes. Noteworthy is the similarity between the six-membered pericyclic transition state in this pathway (**TS2-2**) and those proposed in related H_2 heterolysis, e.g., by mononuclear amido complexes with a solvent alcohol molecule (Chart 1c).[1,3,19] The proton relay from the sulfonyl O atom to the imido N atom and the following spontaneous hydride migration in the hydride−amide intermediate **A** highlight the significance of the Brønsted basicity of the two bridging sulfonylimido nitrogen atoms in this transformation.

Reaction of Bis(amido) Complex 2 with O_2. While the bis(amido)-bridged dirhodium(II) complex **2** is thermally stable in solution even under the reduced pressure, exposure of a dichloromethane solution of **2** to O_2 resulted in rapid formation of the bis(imido)-bridged dirhodium(III) complex **1a** and water (Scheme 5). Although no intermediate has yet been observed, the oxidation seems to occur via initial insertion of O_2 into the Rh(II)−Rh(II) bond in **2**[20] followed by an intramolecular proton shift from the amido ligand to the μ-peroxo ligand as shown in Scheme 5. Tejel and co-workers have demonstrated that protonation of a μ-O_2 complex affords a (μ-1κO,2$\kappa O'$-hydroperoxo)dirhodium complex.[21,22] Regeneration of the bis(imido) complex **1a** from this hydroperoxo intermediate may be explained by scission of the Rh−OOH bond aided by the NHTs proton to yield H_2O_2, which reacts with **2** to give **1a** and H_2O.[23] An alternative scenario that merits comments involves the reaction of the hydroperoxo intermediate with **2** to provide the hydroxo intermediate [(Cp*Rh)$_2$(μ-NHTs)(μ-NTs)(μ-OH)], **1a**, and water; the intermediate then loses water to give **1a**. In this connection, we[23,24] and others[25] recently reported the catalytic aerobic oxidation of alcohols and H_2, which may involve the hydroperoxo intermediates [Cp*Ir(OOH)(L−NH_2)] (L−NH_2 = chelate amine ligands, L denotes monoanionic C and N donors; vide infra).

Table 2. Aerobic Oxidation of H_2

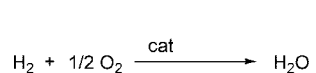

cat	TON[a]
1a	9 (26)[b]
1b	0
[Cp*RhCl$_2$]$_2$	0

[a] Defined as moles of H_2O per mole of the catalyst and determined by ^{1}H NMR spectroscopy. [b] After 169 h.

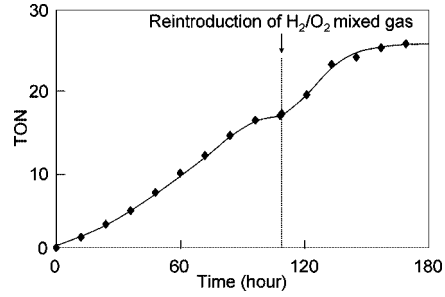

Figure 4. Time course for the catalytic aerobic oxidation of H_2 with **2a**. TON is defined as moles of H_2O per mole of the catalyst.

In contrast to the dirhodium(II) complex **2**, the cationic (hydrido)dirhodium(III) complex **5** failed to react with O_2 under the same conditions.

Catalytic Aerobic Oxidation of H_2 and Alcohol. The facile redox interconversion between **1a** and **2** (Schemes 2 and 5) could be applied to the catalytic aerobic oxidation of H_2 and alcohols. When a CD_2Cl_2 solution of **1a** was treated with a 1:1 mixture of H_2 and O_2 (total pressure: 1 atm), water was produced catalytically (Table 2). In the reaction mixture, the sole rhodium species detectable by ^{1}H NMR spectroscopy is the bis(imido) complex **1a**, suggesting that the rate-determining step is the hydrogenation of **1a**. The turnover number seems limited by consumption of the gases and mass transfer since the rate of the reaction was revived upon addition of H_2 and O_2 (Figure 4).

Although such H_2 oxidation with O_2 promoted by homogeneous catalysts itself is not directly related to the practical energy production, it may provide some clue to the development of proton-coupled electron-transfer catalysts with high efficiency and reversibility. Heiden and Rauchfuss[25] recently reported the aerobic oxidation of H_2 catalyzed by the coordinatively unsaturated (amido)iridium(III) complex [Cp*Ir{TsNCH(C_6H_5)CH(C_6H_5)NH}] with the aid of 10 mol % of a Brønsted acid, possibly to promote the step of H_2 heterolysis;[26] the O_2 hydrogenation is proposed to occur via insertion of O_2 into the Ir−H bond as mentioned above. In contrast, the aerobic H_2 oxidation shown in Table 2 is achieved by direct interconversion between the imido complex **1a** and the amido complex **2** without hydrido ligands. Lacking a facile hydrogenation process, the

(19) (a) Ito, M.; Hirakawa, M.; Murata, K.; Ikariya, T. *Organometallics* **2001**, *20*, 379. (b) Hedberg, C.; Källström, K.; Arvidsson, P. I.; Brandt, P.; Andersson, P. G. *J. Am. Chem. Soc.* **2005**, *127*, 15083. (c) Noyori, R.; Ohkuma, T. *Angew. Chem., Int. Ed.* **2001**, *40*, 40. (d) Clapham, S. E.; Hadzovic, A.; Morris, R. H. *Coord. Chem. Rev.* **2004**, *248*, 2201. (e) Crabtree, R. H.; Siegbahn, P. E. M.; Eisenstein, O.; Rheingold, A. L.; Koetzle, T. F. *Acc. Chem. Res.* **1996**, *29*, 348.

(20) Hoard, D. W.; Sharp, P. R. *Inorg. Chem.* **1993**, *32*, 612.

(21) Tejel, C.; Ciriano, M. A.; Jiménez, S.; Passarelli, V.; López, J. A. *Angew. Chem., Int. Ed.* **2008**, *47*, 2093.

(22) We note that recent studies suggest that an oxidized, unready state of [NiFe]-hydrogenases called Ni-A contains a bridging hydroperoxo ligand.[2]

(23) Arita, S.; Koike, T.; Kayaki, Y.; Ikariya, T. *Angew. Chem., Int. Ed.* **2008**, *47*, 2447.

(24) Arita, S.; Koike, T.; Kayaki, Y.; Ikariya, T. *Chem. Asian J.* **2008**, *3*, 1479.

(25) Heiden, Z. M.; Rauchfuss, T. B. *J. Am. Chem. Soc.* **2007**, *129*, 14303.

Table 3. Aerobic Oxidation of Alcohol

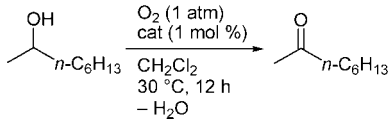

cat	TON[a]
1a	15
1b	0
$[Cp^*RhCl_2]_2$	0

[a] Determined by GC.

iridium analogue **1b** and a rhodium complex $[Cp^*RhCl_2]_2$ without bridging imido ligands did not catalyze the oxidation at all.

The sulfonylimido-bridged dirhodium complex **1a** also catalyzes the aerobic dehydrogenative oxidation of alcohols. Reaction of 2-octanol with O_2 (1 atm) proceeded in the presence of 1 mol % of **1a** at 30 °C to give 2-octanone as shown in Table 3. Again, the iridium complex **1b** and a rhodium complex $[Cp^*RhCl_2]_2$ without bridging imido ligands did not show any catalytic activity, indicating that the reaction takes place via the imido−amido interconversion shown in Schemes 2 and 5. Aerobic oxidation of alcohols has been extensively studied as a clean and environmentally benign process.[27] We have recently reported the aerobic oxidation of alcohols[24] and even the oxidative kinetic resolution of racemic alcohols[23] promoted by the mononuclear chelating amido complexes with the metal−nitrogen bifunction. It is noteworthy that the catalysis shown in Table 3 additionally involves the redox of the dirhodium center, and to the best of our knowledge, **1a** represents the first well-defined dinuclear catalyst for this reaction without fragmentation throughout the catalysis.

Conclusion

We have demonstrated that H_2 is converted into two protons and two electrons on the sulfonylimido-bridged dirhodium(III) complex **1a**. The sulfonyl groups apparently balance the basicity of the metal center and the bridging ligands delicately[10,11] to facilitate the heterolysis of H_2 and hydride migration leading to the separation of the protons and electrons. Importantly, the two protons and two electrons thus generated in **2** can be removed by proton-coupled electron transfer to O_2,[28] to regenerate the (imido)dirhodium(III) complex **1a**. Based on the facile interconversion between **1a** and **2**, catalytic aerobic oxidation of H_2 and alcohols is achievable under mild conditions. Effort will be directed to the development of catalysis featuring the redox-coupled acid−base bifunction of the sulfonylimido-bridged dinuclear complexes. Further mechanistic elucidation of the aerobic oxidation of the amido-bridged dirhodium(II) complex **2** is also under way.

Experimental Section

General Procedures. All manipulations were performed under an atmosphere of argon using standard Schlenk techniques. Solvents were dried by refluxing over sodium benzophenone ketyl (THF, toluene, hexane, diethyl ether) and CaH_2 (CH_2Cl_2, 2-propanol) and stored under an atmosphere of argon. Reagents were purchased from Kanto Chemicals, Aldrich, Tokyo Kasei Industry, Wako or Fluka. ^1H (300.40 and 399.78 MHz) NMR spectra were obtained on a JEOL JNM-LA300 and JNM-ECX400 spectrometer. ^1H NMR shifts are relative to the residual protiated solvent: $CHCl_3$, δ 7.26; $CDHCl_2$, δ 5.32; C_6D_5H, δ 7.15. ^{19}F NMR shifts are relative to an external CF_3COOH. IR spectra were recorded on a JASCO FT/IR-610 spectrometer. GC analyses were carried out using a Shimadzu GC-17A with an INNOWAX column. Elemental analyses were performed on a Perkin-Elmer 2400II CHN analyzer or by the Analytical Facility at the Research Laboratory of Resources Utilization, Tokyo Institute of Technology.

Preparation of $[(Cp^*Rh)_2(\mu\text{-}NTs)_2]$ (1a). A mixture of $[Cp^*RhCl_2]_2$ (2.0000 g, 3.2359 mmol),[29] $TsNH_2$ (1.1098 g, 6.4817 mmol), and KOH (1.4567 g, 25.962 mmol) in CH_2Cl_2/H_2O (20 mL/20 mL) was stirred for 3 h at room temperature. The resultant organic layer was separated, washed with H_2O (20 mL × 5), and evaporated to dryness. The resultant solid was recrystallized from CH_2Cl_2/hexane (15 mL/70 mL) to yield **1a** as dark violet crystals (2.4441 g, 3.0001 mmol, 93%). ^1H NMR (C_6D_6): δ 8.10, 6.88 (d, 4H each, J = 8.1 Hz, $SO_2C_6H_4CH_3$), 2.00 (s, 6H, $SO_2C_6H_4CH_3$), 1.52 (s, 30H, Cp*). Anal. Calcd for $C_{34}H_{44}N_2O_4Rh_2S_2$: C, 50.13; H, 5.44; N, 3.44. Found: C, 50.26; H, 5.45; N, 3.43.

Preparation of $[(Cp^*Rh)_2(\mu\text{-}NHTs)_2]$ (2). A CH_2Cl_2 (5 mL) solution of **1a** (40.0 mg, 0.0491 mmol) in a Schlenk tube was degassed by three freeze−pump−thaw cycles. H_2 (1 atm) gas was introduced to the Schlenk tube, and the mixture was stirred for 24 h at room temperature. After removal of the solvent in vacuo, the resultant solid was extracted with toluene (3 mL). Addition of hexane (5 mL) to the concentrated extract (ca. 0.1 mL) and cooling the mixture at 2 °C yielded **2** as a dark purple solid (32.9 mg, 0.0403 mmol, 82%). ^1H NMR (C_6D_6): δ 8.18, 7.92 (d, 2H each, J = 8.2 Hz, $SO_2C_6H_4CH_3$), 6.84, 6.83 (d, 2H each, J = 7.8 Hz, $SO_2C_6H_4CH_3$), 5.46, 2.53 (s, 1H each, NH), 1.93, 1.92 (s, 3H each, $SO_2C_6H_4CH_3$), 1.59 (s, 30H, Cp*). IR (KBr): 3207 cm^{-1} (ν_{NH}). Anal. Calcd for $C_{34}H_{46}N_2O_4Rh_2S_2$: C, 50.00; H, 5.68; N, 3.43. Found: C, 49.71; H, 5.72; N, 3.36.

Conversion of 1a to 2 with 2-Propanol. To a solution of **1a** (100.0 mg, 0.123 mmol) in CH_2Cl_2 (5 mL) was added 2-propanol (93.4 μL, 1.23 mmol), and the mixture was stirred for 16 h at room temperature. After removal of the solvent in vacuo, the resultant solid was extracted with toluene (3 mL). Addition of hexane (5 mL) to the concentrated extract (ca. 0.1 mL) and cooling the mixture at 2 °C yielded **2** as dark purple solid (76.4 mg, 0.0935 mmol, 76%).

Preparation of 2·$TsNH_2$ from 1a and 2-Propanol. A mixture of **1a** (81.4 mg, 0.0999 mmol) and $TsNH_2$ (17.1 mg, 0.0999 mmol) in 2-propanol−CH_2Cl_2 (1 mL/4 mL) was stirred for 15 h at room temperature. The resultant purple solution was concentrated to ca. 1 mL. Slow addition of hexane (20 mL) and cooling the mixture at −30 °C yielded **2**·$TsNH_2$ as dark purple crystals (74.1 mg, 0.075 mmol, 75%). Anal. Calcd for $C_{41}H_{55}N_3O_6Rh_2S_3$: C, 49.85; H, 5.61; N, 4.25. Found: C, 50.01; H, 5.68; N, 4.16.

Interconversion between 1a and 2. To a solution of **1a** (4.8 mg, 0.0059 mmol) in CD_2Cl_2 (0.5 mL) with durene as an internal standard was added 2-propanol (2.7 μL, 0.035 mmol). After 16 h, **1a** was converted to **2** (99% based on **1a**) and an equimolar amount of acetone was observed. Then, the solution was degassed by three freeze−pump−thaw cycles. Spontaneous conversion to **1a** was not observed at this stage. Subsequent introduction of oxygen (1 atm) to the tube afforded **1a** (62% based on the starting **1a**) immediately.

Preparation of $[(Cp^*Rh)_2(\mu\text{-}NHTs)(\mu\text{-}NTs)][OTf]$ (4). To a solution of **1a** (400.0 mg, 0.491 mmol) in CH_2Cl_2 (10 mL) was added HOTf (43.4 μL, 0.491 mmol), and the mixture was stirred for 1 h at room temperature. The resultant dark brown solution

(26) (a) Heiden, Z. M.; Rauchfuss, T. B. *J. Am. Chem. Soc.* **2006**, *128*, 13048. (b) Sandoval, C. A.; Ohkuma, T.; Utsumi, N.; Tsutsumi, K.; Murata, K.; Noyori, R. *Chem. Asian J.* **2006**, *1*−*2*, 102. (c) Ohkuma, T.; Utsumi, N.; Tsutsumi, K.; Murata, K.; Sandoval, C.; Noyori, R. *J. Am. Chem. Soc.* **2006**, *128*, 8724.

(27) (a) Sigman, M. S.; Jensen, D. R. *Acc. Chem. Res.* **2006**, *39*, 221. (b) Schultz, M. J.; Sigman, M. S. *Tetrahedron* **2006**, *62*, 8227. (c) Stahl, S. S. *Angew. Chem., Int. Ed.* **2004**, *43*, 3400. (d) Conley, N. R.; Labios, L. A.; Pearson, D. M.; McCrory, C. C. L.; Waymouth, R. M. *Organometallics* **2007**, *26*, 5447. (e) Jiang, B.; Feng, Y.; Ison, E. A. *J. Am. Chem. Soc.* **2008**, *130*, 14462. (f) Ebner, D. C.; Trend, R. M.; Genet, C.; McGrath, M. J.; O'Brien, P.; Stoltz, B. M. *Angew. Chem., Int. Ed.* **2008**, *47*, 6367.

(28) Rosenthal, J.; Nocera, D. G. *Acc. Chem. Res.* **2007**, *40*, 543.

(29) White, C.; Yates, A.; Maitlis, P. M. *Inorg. Synth.* **1992**, *29*, 230.

was concentrated to ca. 1 mL. Slow addition of diethyl ether (15 mL) and cooling the mixture at 2 °C yielded **4** as dark brown crystals (469.4 mg, 0.487 mmol, 99%). ^{1}H NMR (C_6D_6): δ 8.46 (s, 1H, NH), 8.44, 8.26, 6.88 (d, 2H each, J = 8.2 Hz, $SO_2C_6H_4CH_3$), 1.95, 1.91 (s, 3H each, $SO_2C_6H_4CH_3$), 1.37 (s, 30H, Cp*). The signal for the rest aryl proton is overlapped by the solvent signal. ^{19}F{^{1}H} NMR (C_6D_6): δ −78.1 (s). IR (KBr): 3160 cm^{-1} (ν_{NH}). Anal. Calcd for $C_{35}H_{45}F_3N_2O_7Rh_2S_3$: C, 43.57; H, 4.70; N, 2.90. Found: C, 43.43; H, 4.81; N, 2.84.

Conversion of 4 to 1a. A mixture of **4** (12.0 mg, 0.0124 mmol) and KOH (2.5 mg, 0.0446 mmol) in CH_2Cl_2 (2 mL) was stirred for 8 h at room temperature. The resultant violet solution was filtrated off and concentrated to ca. 1 mL. Slow addition of hexane (10 mL) and cooling the mixture at 2 °C yielded **1a** as dark violet crystals (7.7 mg, 0.0095 mmol, 76%).

Conversion of 4 to 2. To a solution of **4** (50.0 mg, 0.0518 mmol) in CH_2Cl_2 (5 mL) was added a THF solution of $LiBH(C_2H_5)_3$ (1.0 M, 51.8 μL, 0.0518 mmol) at 0 °C. The reaction mixture was slowly warmed to room temperature with stirring. After 3 h, the resultant purple solution was evaporated to dryness and the resultant solid was extracted with toluene (3 mL). Addition of hexane (5 mL) to the concentrated extract (ca. 0.1 mL) and cooling the mixture at 2 °C yielded **2** as a dark purple solid (24.2 mg, 0.0296 mmol, 57%).

Preparation of [(Cp*Rh)$_2$(μ-NHTs)$_2$(μ-H)][OTf] (5). To a solution of **1a** (300.3 mg, 0.3686 mmol) in CH_2Cl_2 (6 mL) were added HOTf (32.6 μL, 0.368 mmol) and 2-propanol (2 mL) at 0 °C, and the mixture was slowly warmed to 10 °C with stirring. After 18 h, the resultant red-orange solution was evaporated to dryness. Recrystallization from THF−hexane (2 mL/10 mL) gave **5** as orange crystals (333.9 mg, 0.3454 mmol, 94%). ^{1}H NMR (C_6D_6): δ 8.37, 7.95, 7.09, 6.76 (d, 2H each, J = 8.2 Hz, $SO_2C_6H_4CH_3$), 6.54, 5.58 (s, 1H each, NH), 1.92, 1.88 (s, 3H each, $SO_2C_6H_4CH_3$), 1.55 (s, 30H, Cp*), −9.20 (t, 1H, $^1J_{RhH}$ = 23.3 Hz, RhH). ^{19}F{^{1}H} NMR (C_6D_6): δ −78.4 (s). IR (KBr): 3154 cm^{-1} (μ_{NH}). Anal. Calcd for $C_{35}H_{47}F_3N_2O_7Rh_2S_3$: C, 43.48; H, 4.90; N, 2.90. Found: C, 43.30; H, 4.51; N, 2.82.

Conversion of 2 to 5. To a solution of **2** (34.0 mg, 0.0416 mmol) in CH_2Cl_2 (3 mL) was added HOTf (3.7 μL, 0.0416 mmol), and the mixture stirred for 3 h at room temperature. After removal of the solvent in vacuo, the residue was dissolved in THF (1 mL). Addition of hexane (10 mL) gave **5** as an orange solid (28.1 mg, 0.0291 mmol, 70%).

Conversion of 4 to 5 with H$_2$. A CH_2Cl_2 (5 mL) solution of **4** (40.0 mg, 0.0415 mmol) in a Schlenk tube was degassed by three freeze−pump−thaw cycles. H_2 (1 atm) gas was introduced to the Schlenk tube, and the mixture was stirred for 24 h at room temperature. After removal of the solvent in vacuo, the resultant solid was extracted with THF (2 mL). Addition of diethyl ether (10 mL) to the concentrated extract (ca. 1 mL) and cooling the mixture at 2 °C yielded **5** as an orange solid (25.0 mg, 0.0259 mmol, 62%).

Conversion of 4 to 5 with 2-Propanol. To a solution of **4** (50.0 mg, 0.0518 mmol) in CH_2Cl_2 (5 mL) was added 2-propanol (39.4 μL, 0.518 mmol), and the mixture was stirred for 6 h at room temperature. After removal of the solvent in vacuo, the residue was dissolved in THF (1 mL). Addition of hexane (10 mL) gave **5** as an orange solid (44.4 mg, 0.0459 mmol, 89%).

Conversion of 5 to 2. To a solution of **5** (50.0 mg, 0.0517 mmol) in THF (5 mL) was added a hexane solution of n-C_4H_9Li (1.61 M, 32.0 μL, 0.0515 mmol) at 0 °C. The reaction mixture was warmed to room temperature with stirring and stirred for additional 3 h. After removal of the solvent in vacuo, the resultant solid was extracted with toluene (3 mL). Addition of hexane (5 mL) to the concentrated extract (ca. 0.1 mL) and cooling the mixture at 2 °C yielded **2** as a dark purple solid (20.8 mg, 0.0255 mmol, 49%).

Catalytic Aerobic Oxidation of H$_2$. To an NMR tube equipped with a J-Young valve were added a catalyst (0.6 μmol), hexamethylbenzene (0.2 mg, 1.2 μmol, as an internal standard), and CD_2Cl_2 (0.5 mL), and the mixture was degassed by three freeze−pump−thaw cycles. A 1:1 mixture of H_2 and O_2 (total pressure: 1 atm) gas was introduced to the tube and maintained at 30 °C for 60 h. The reaction was periodically monitored by ^{1}H NMR spectroscopy.

Catalytic Aerobic Oxidation of 2-Octanol. To a 20-mL Schlenk tube were added a catalyst (0.01 mmol), 2-octanol (1.00 mmol), durene (26.8 mg, 0.20 mmol, as an internal standard), and CH_2Cl_2 (1.0 mL), and the mixture was degassed by three freeze−pump−thaw cycles. O_2 (1 atm) gas was introduced to the Schlenk tube, and the mixture was stirred for 12 h at 30 °C. The resultant solution was diluted with CH_2Cl_2 (9.0 mL) and analyzed by GC.

X-ray Diffraction Studies. A single crystal suitable for the X-ray analysis was mounted on a glass fiber. Diffraction experiments were performed on a Rigaku Saturn CCD area detector with graphite monochromated Mo Kα radiation (λ = 0.710 70 Å). Intensity data were corrected for Lorentz polarization effects and for absorption.

Structure solution and refinements were carried out by using the CrystalStructure program package.[30] The heavy-atom positions were determined by a Patterson method program (DIRDIF99 PATTY[31]), and remaining non-hydrogen atoms were found by subsequent Fourier syntheses. One of the two Cp* groups in **2**·$TsNH_2$ as well as the tolyl group in the cocrystallizing $TsNH_2$ was found to be severely disordered. The Cp* group is placed at two disordered positions with a 50% occupancy, and these Cp* groups as well as the partially disordered tolyl group have been included in the refinements as rigid groups with isotropic thermal parameters. The rest of the non-hydrogen atoms were refined anisopropically by full-matrix least-squares techniques based on F^2. All hydrogen atoms except for those in the disordered groups were placed at calculated positions and included in the final stages of the refinements. The atomic scattering factors were taken from ref 32, and anomalous dispersion effects were included; the values of $\Delta f'$ and $\Delta f''$ were taken from ref 33. Crystal data for **2**·$TsNH_2$: $C_{41}H_{55}N_3O_6Rh_2S_3$, FW = 987.89, triclinic, $P\bar{1}$, dark purple, a = 10.696(9) Å, b = 11.903(9) Å, c = 17.801(14) Å, α = 96.228(13)°, β = 102.202(12)°, γ = 99.063(14)°, V = 2164(3) Å^3, T = 193 K, Z = 2, $R1$ = 0.107 [$I > 2\sigma(I)$], w$R2$ = 0.238 (all data), GOF = 1.006.

Computational Studies. All calculations were performed using the density functional theory in the Gaussian 03 program.[34] The entire reaction pathway and relative energy barriers for each step are obtained by use of an exchange-correlation hybrid functional, denoted as MPW1PW91. For this density functional method, the correlation functional is from Perdew−Wang 1991 (PW91),[35] while the exchange functional is from Barone's modified PW91 (MPW1).[36] For the basis set, the rhodium atoms were represented by LANL2DZ (Los Alamos effective core potential plus double-ζ), while the other atoms were represented by 6-31G(2d,p). All the geometry structures are fully optimized by closed-shell spin-restricted calculations using the MPW1PW91 functional and LANL2DZ (Rh)/6-31G(2d,p) basis sets. The structural optimization of **1a′** and the bis(amido) complex [(Cp*Rh)$_2$(μ-NHMs)$_2$] (**2a′**) reproduced the geometrical characteristics of **1a** and **2** determined by X-ray analyses. Calculating the harmonic vibrational frequencies and noting the number of imaginary frequencies confirmed the

(30) *CrystalStructure 3.8: Crystal Structure Analysis Package*; Rigaku and Rigaku/MSC: The Woodlands, TX 77381, USA, 2000−2006.
(31) DIRDIF99: Beurskens, P. T.; Admiraal, G.; Beurskens, G.; Bosman, W. P.; de Gelder, R.; Israel, R.; Smits, J. M. M. *The DIRDIF-99 program system*; Technical Report of the Crystallography Laboratory; University of Nijmegen: The Netherlands, 1999.
(32) *International Tables for X-ray Crytallography*; Kynoch Press: Birmingham, U.K., 1974; Vol. IV.
(33) *International Tables for X-ray Crytallography*; Kluwer Academic Publishers: Boston, MA, 1992; Vol. C.
(34) Frisch, M. J. et al. *Gaussian03*, revision C.02; Gaussian, Inc.: Wallingford, CT, 2004.
(35) Perdew, J. P.; Wang, Y. In *Electronic Structures of Solids 91*; Ziesche, P., Eschrig, H., Eds.; Akademie-Verlag: Berlin, 1991.
(36) Adamo, C.; Barone, V. *Chem. Phys. Lett.* **1997**, *274*, 242.

nature of all intermediates (NImag = 0) and transition state structures (NImag = 1), which also were confirmed to connect reactants and products by the intrinsic reaction coordinate (IRC) calculations. The zero-point energy (E_0) and entropic contribution have been estimated within the harmonic potential approximation. The enthalpies, H, and free energies, G, were calculated for T = 298.15 K. All relative zero-point energies, enthalpies, and free energies are reported in kcal/mol, where separated molecules [(Cp*Rh)$_2$(μ-NMs)$_2$] (**1a′**, **GS**) and H_2 are set equal to 0.0 kcal/mol. Relative stabilities of the ground states and transition states were discussed on the basis of the free energies. Figures of the molecular structures are drawn by using GaussView 4.1.[37]

Acknowledgment. This work was supported by a Grant-in-Aid for Scientific Research on Priority Areas (No. 18065007, "Chemistry of *Concerto* Catalysis") from the Ministry of Education, Culture, Sports, Science and Technology, Japan.

Supporting Information Available: X-ray crystallographic data for **2**·TsNH$_2$. Atomic Cartesian coordinates for all the structures optimized in the DFT calculations. Complete ref 34. This material is available free of charge via the Internet at http://pubs.acs.org.

JA900650J

(37) Dennington, R., II; Keith, T.; Millam, J . *GaussView*, version 4.1.2; Semichem, Inc.: Shawnee Mission, KS, 2007.